P8.3 DYNAMICS OF THE SURFACE LAYER OVER THE OCEAN AS REVEALED FROM FIELD MEASUREMENTS OF THE ATMOSPHERIC PRESSURE

Tihomir Hristov[1,*], Kenneth Anderson[2], James Edson[3] and Carl Friehe[4]

[1] *Dept. of Earth and Planetary Sciences, Johns Hopkins University, Baltimore, Maryland*
[2] *SPAWARSYSCEN-SD, 2858, San Diego, California*
[3] *Woods Hole Oceanographic Institution, Woods Hole, Massachusetts*
[4] *Dept. of Mechanical and Aerospace Engineering, Univ. of California, Irvine, California*

1. INTRODUCTION

The spatio-temporal structure of the pressure field in the atmospheric boundary layer is a significant element in the layer's dynamics. Pressure affects the atmospheric refractive conditions, thus pressure statistics is required in studies of electromagnetic propagation. Although indirect experimental estimates and models have suggested important role for the pressure field both over land and over the ocean, infrequent measurements have so far provided only scarce data (Wyngaard (1998)).

In turbulent boundary layers, the kinetic energy (TKE) is balanced through the pressure transport $\rho^{-1}\partial_z\langle pw\rangle$. A belief commonly shared before the Kansas experiment has been that the pressure transport term is small. However, indirect estimates as well as direct pressure measurements have indicated that over land the pressure transport can be a significant TKE gain if the surface layer is unstable (Wyngaard (1992, 1998)). Over the ocean the atmospheric surface layer is modified by the presence of ocean waves, as shown by wind velocity analysis of Hristov et al. (1998, 2003). The distribution of air pressure on the water surface determines the rate of kinetic energy transfer from wind to the surface waves. Consequently, past experiments have conducted direct measurements of the interfacial pressure (Shemdin and Hsu (1967); Dobson (1971); Elliott (1972); Snyder (1974); Snyder et al. (1981)) or have considered extrapolated estimates Papadimitrakis et al. (1986); Hasselmann and Bösenberg (1991); Hare et al. (1997); Donelan (1999). However, the interfacial pressure distribution does not specify the spatio-temporal structure of the wave-induced air flow, which uniquely selects the physical mechanism of wind-wave coupling. Experimental determination of that structure requires measurements in the surface layer over the ocean.

Broadly, the wind-wave interaction models and theories proposed so far have considered two categories of physical mechanisms. The Phillips (1957) theory relies on the turbulent pressure fluctuations to provide a random (Langevin) force acting onto the water surface that ensures wind-to-wave energy transfer. Fields in the wind correlated with the water surface motion are considered negligible and are ignored. Within this model the wave amplitude increases linearly in time, thus evolving in a way similar to a Brownian particle driven by the random forcing from its surrounding particles. The most efficient wind-to-wave energy transfer is found to occur from a pressure component advected with the wave and having the same wavenumber. Several theories for wind-wave interaction (Miles (1957); Davis (1969); Belcher and Hunt (1993)), although differing in their details, are built on the concept of fluid-mechanical instability. In that concept the waves perturb the mean air flow and the turbulence in the wind, so the perturbation provides the feedback from wind to waves ensuring wave growth. Numerical models (Gent and Taylor (1976); Chalikov and Makin (1991); Meirink and Makin (2000)) have also employed such a concept, while direct numerical simulations have arrived to it (Sullivan et al. (2000); Sullivan and McWilliams (2002)).

Observations have so far provided limited information on the physics of wind-wave interaction. Particularly, the random force mechanism has never been addressed experimentally. Here the basic distinction between the way the random force and the instability mechanisms operate, is used to formulate an experimental criterion for their relative efficiency. The random force mechanism requires that the pressure field in the wind is predominantly turbulent, while, in contrast, the instability mechanism relies on the organized wave-induced fields of velocity and pressure in the air. Therefore, to compare the efficiency of the random force versus the instability mechanism, we need to compare the intensities of the turbulent and wave-induced pressure in the air flow. On the other hand, recognizing a particular instability mechanism in measured data requires finding an agreement between the theoretically predicted and the observed structure of the wave-induced flow (Hristov et al. (2003)).

In this work, from experimental perspective, we address the relative intensity of random force and instability mechanisms. We also discuss the issue of TKE balance

*Corresponding author address: Tihomir Hristov, Department of Earth and Planetary Sciences, Johns Hopkins University, 3400 North Charles Str., Baltimore, MD 21218, e-mail: Tihomir.Hristov@jhu.edu

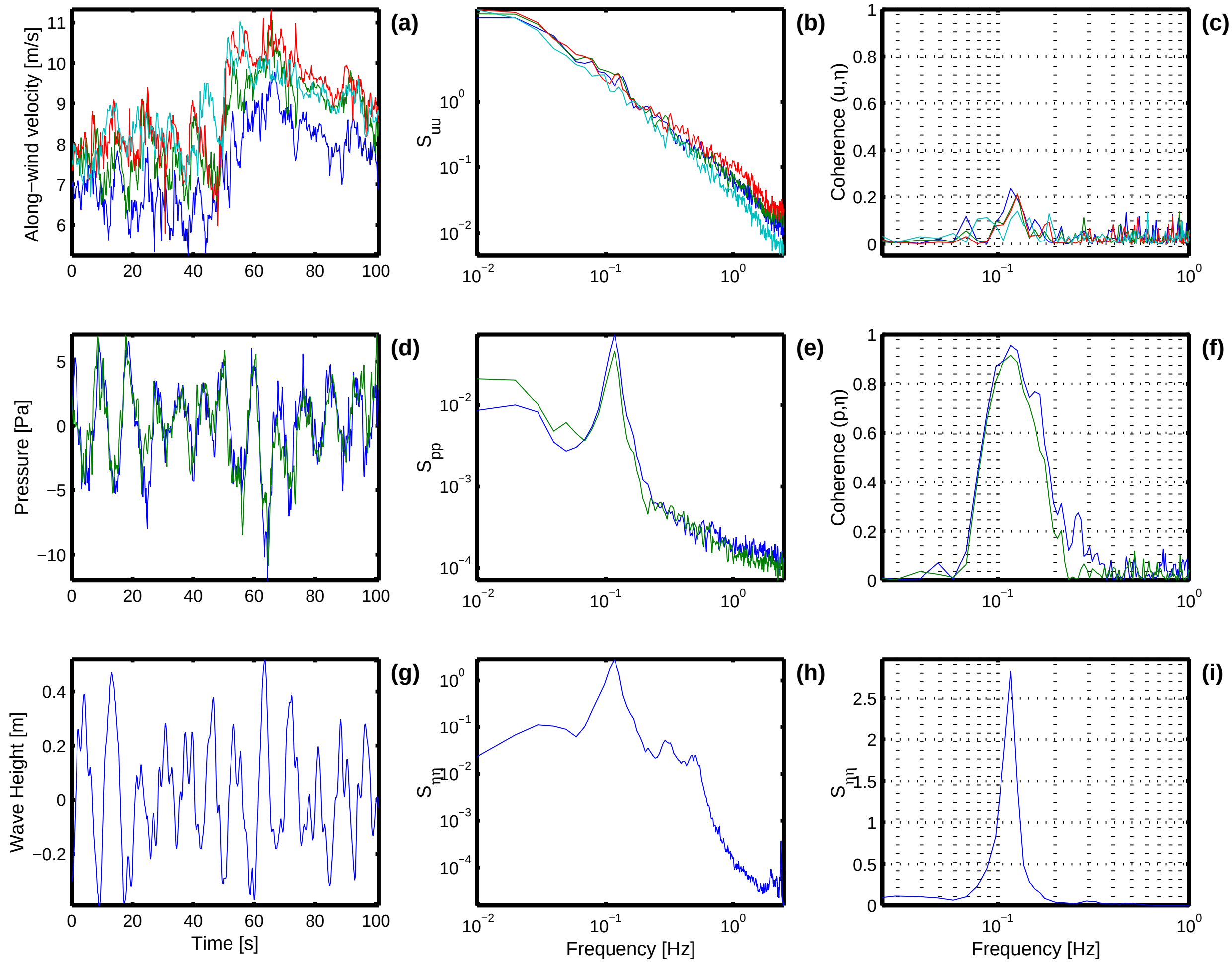

Figure 1: *A flow regime frequently observed during CBLAST. (a) Timeseries of along-wind air velocities from the four ultrasonic anemometers over 100s; (b) Power spectra of along-wind air velocities calculated from 1 hour of data; (c) coherence between the along-wind air velocities and the surface elevation; (d) timeseries of the atmospheric pressure fluctuations at 2 levels; (e) pressure fluctuations power spectra calculated from 1 hour of data; (f) coherence between the pressure fluctuations and the surface elevation; (g) timeseries of the water surface elevation; (h) and (i) power spectra of the water surface elevation.*

over the ocean in the context of our experimental data.

2. EXPERIMENTAL SETTING

The data analyzed here were collected at the WHOI-operated Air-Sea Interaction Tower (ASIT) off the coast of Massachusetts. Four sonic anemometers sampled the wind velocity at 20Hz at levels of 7.2m, 9m, 11m, 13.4m above the ocean surface. Two pressure sensors were positioned at heights of 9m and 11m. A TSK instrument measured remotely the water surface elevation beneath the sonic anemometers and pressure sensors. Data were collected continuously from late June through early November of 2003. For most of that period winds ranged between 1 and 12 m/s and significant wave heights were below 1.5m, except for short storm periods when winds reached 20m/s and significant wave heights exceeded 3m. Instances of flow distortion from the tower are relatively rare, although very clear in the data. Rain occasionally disrupted the sonic anemometers work.

3. DATA INTERPRETATION

Figure 1 summarizes the features of a flow regime frequently observed during the experiment. The data show that the along-wind velocity is mostly turbulent, as indicated by the timeseries and the power spectra, with some suggestion of small wave influence in the coherence function. In contrast, the pressure appears almost entirely organized and modulated by the waves. Comparing the pressure and the wave height signals, it is clearly noticeable that the wave crests approximately coincide in time with the minima and the troughs with the maxima of the pressure. A distinct peak at the wave frequency is present over the turbulent background in the pressure. The wave-pressure coherence, which here compares the intensities of the wave-induced and the turbulent pressure, approaches 1 and is significant over a broad frequency range even for low-energy wave modes. Clearly, the data demonstrate that in the wind the organized wave-induced pressure dominates and therefore in this flow regime the instability mechanism of wind-wave interaction is favored to the mechanism of random (Langevin) force. Two circumstances discussed below offer a likely explanation. Also, predominantly wave-modulated pressure suggests an analytic estimate for the pressure transport term in the TKE equation.

4. DISCUSSION

If a flow allows to ignore the fluid's compressibility, the static pressure in that flow satisfies the Poisson equation:

$$\nabla^2 p = -\nabla \cdot (\mathbf{v} \cdot \nabla)\mathbf{v}.$$

From here, extending Kolmogorov's arguments regarding the spectral scaling of the turbulent velocity to the turbulent pressure leads to the conclusion that turbulent pressure spectrum decays with scale as $F_p(k) \sim k^{-7/3}$, i.e. faster than velocity's spectral decay of $F_u(k) \sim k^{-5/3}$. Let us introduce the wavenumber corresponding to the integral scale in the atmospheric boundary layer, $k_{\rm int}$, the variance of a turbulent quantity X retained by wavenumbers k and larger, $V_X(k) \equiv \int_k^\infty F_X(q)\mathrm{d}q$ and let $k_{\rm wave}$ denote a representative wavenumber for the ocean surface waves. For typical conditions $k_{\rm wave}/k_{\rm int} \geq 10^2$. Thus for wavenumbers $k_{\rm wave}$ and larger the turbulent velocity field u retains a variance fraction $V_u(k_{\rm wave})/V_u(k_{\rm int}) = (k_{\rm wave}/k_{\rm int})^{-2/3}$, while the turbulent pressure retains a considerably smaller variance fraction, $V_p(k_{\rm wave})/V_p(k_{\rm int}) = (k_{\rm wave}/k_{\rm int})^{-4/3}$.

A previous field experiment (Hristov et al. (2003)) has found a good agreement between the observed structure of the wave-induced flow and the one predicted by the critical layer theory of Miles (1957). This gives us some confidence in the theory's description of the wave-induced fields. In this theory the turbulence in the wind is responsible for creating a constant-stress layer over the ocean with averaged flow velocity obeying the law of the wall, i.e. $U(z) = (u_*/\kappa)\log(z/z_0)$. The perturbation of the equilibrium flow $U(z)$ by the waves is governed by the Rayleigh equation with controlling parameter (c/u_*), known as wave age. Important dynamic significance is assigned to the critical height z_c, where the wind speed matches the phase speed c of the considered wave mode, i.e. where $U(z) - c = (u_*/\kappa)\log(z/z_c) = 0$. Figure 2 presents numerical solutions of the Rayleigh equation for the wave-induced along-wind velocity $\tilde{u}$ and the static pressure $\tilde{p}$. The solutions predict a distinctly different behavior of the fields $\tilde{u}(z)$ and $\tilde{p}(z)$. While the velocity $u(z)$ shows considerable decay with z, for a broad range of wave ages (c/u_*) the pressure remains virtually unchanged both in amplitude and phase. Therefore, almost unattenuated surface value of the wave-induced

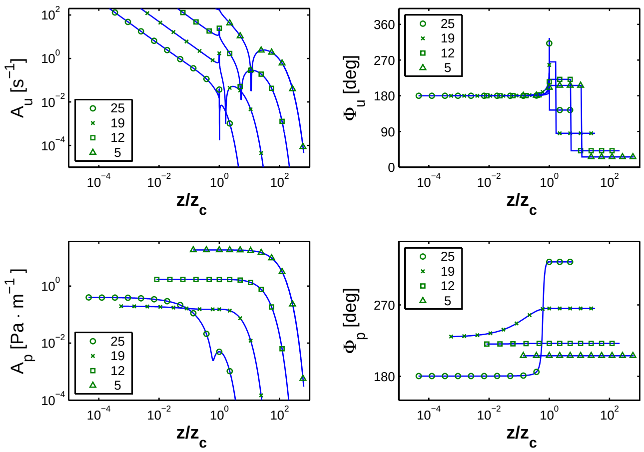

Figure 2: *Vertical profiles of the wave-induced along-wind and pressure fluctuations obtained from numerical solutions of the Rayleigh equation, according to the critical layer theory of Miles (1957). Different curves correspond to specific values of the wave age parameter c/u_*, as indicated in the symbol list. The amplitude $A_{\tilde{u}}$ of the along-wind velocity fluctuations (upper left), the phase $\Phi_{\tilde{u}}$ of the along-wind velocity fluctuations (upper right), the amplitude $A_{\tilde{p}}$ of the pressure fluctuations (lower left), the pressure fluctuations phase $\Phi_{\tilde{p}}$ (lower right). z_c is the critical height.*

pressure is projected vertically beyond the height z_c.

The pressure transport term $\rho^{-1}\partial_z\langle pw\rangle$ in the TKE equation has often been considered small and due to the lack of pressure measurements that term has been estimated as a residual of all the other terms. The observation that the pressure field over the waves is predominantly organized suggests a corollary regarding the pressure transport there. Let us present the pressure p and the vertical velocity w fluctuations in the wind as consisting of turbulent $\{p', w'\}$ and wave-coherent components $\{\tilde{p}, \widetilde{w}\}$, i.e. $p = p' + \tilde{p}$ and $w = w' + \widetilde{w}$. Since most of the pressure signal is wave-coherent, i.e. $\langle (p')^2\rangle \ll \langle (\tilde{p})^2\rangle$ and therefore $p \approx \tilde{p}$, that wave-coherent pressure will correlate only with the wave-coherent vertical velocity $\widetilde{w}$, i.e. $\langle pw\rangle \approx \langle \tilde{p}\widetilde{w}\rangle$. Relaying again on the shear flow instability model (Lin (1955); Miles (1957)), the wave-induced pressure $\tilde{p}$ and velocities $\{\tilde{u}, \widetilde{w}\}$ are related by

$$\tilde{p} = (\rho_a u_*/\kappa)\left(-\xi\tilde{u} + \mathrm{i}\Omega^{-1}\xi_0^2 e^{\xi_0-\xi}\widetilde{w}\right), \qquad (1)$$

where ρ_a is the air density, u_* is the turbulent friction velocity, κ is the von Karman's constant, Ω is the Charnok's parameter, $\xi \equiv \log(z/z_c)$, $\xi_0 \equiv \log(z_0/z_c) = -\kappa c/u_*$, z is the coordinate in vertical direction, and $z_0 = \Omega u_*^2/(g\kappa^2)$ is the sea surface roughness. From here, the real part of the "pressure flux" is expressed as

$$\Re(\tilde{p}\widetilde{w}) = -\frac{\rho_a u_*}{\kappa}\xi(\tilde{u}\widetilde{w}^* + \tilde{u}^*\widetilde{w}) = -\frac{2u_*}{\kappa}\xi\,\tau(z, c/u_*), \qquad (2)$$

$\tau(z, c/u_*)$ being the wave-coherent momentum flux associated with the wave mode of phase speed c. Integrating

$\tau(z, c/u_*)$ over the wave spectrum of all phase speeds c, we obtain for the pressure transport term:

$$\partial_z \langle p'w' \rangle \approx \partial_z \langle \tilde{p}\tilde{w} \rangle = \left(\frac{u_*}{\kappa z}\right) \Upsilon, \qquad (3)$$

where Υ stands for the total wave-induced momentum flux, i.e. the momentum flux associated with the whole wave spectrum. Since the critical layer theory is a linear one, the amount and the spectral distribution of energy in the wave field determines the magnitude of the wave-induced momentum flux. In conditions with low intensity of the wind turbulence air motion is substantially wave-driven and the wave-coherent momentum flux can exceed 50% of the total momentum flux. In conditions with high turbulent intensity, and especially when the wave field is not yet developed, at the heights of our instruments the wave-induced momentum flux is a smaller fraction (1% to 10%) of the total momentum flux.

5. SUMMARY

In theoretical and numerical studies two types of physical mechanisms have been employed in describing wind-wave interaction: the mechanism of random force (Langevin force) and the mechanism of fluid-mechanical instability. Measurements of wind velocity and atmospheric pressure presented here illustrate a frequently observed air flow regime where the velocity is dominated by turbulence, while the pressure is mostly organized and correlated with waves. Such flow structure clearly favors the instability mechanism of wind-wave interaction. We consider two circumstances that lead to and may explain such organized-pressure flow regime. First, the turbulent cascade delivers little pressure variance (much less than velocity variance) at scales of the surface waves' wavelengths. Second, theory predicts substantial decay for the organized velocity with height, while the organized pressure remains unattenuated up to the critical height z_c. Considering the strong organized component in the pressure signal, we proposed an analytical estimate of the pressure transport term through the wave-coherent momentum flux.

Acknowledgments. Discussions with O. Phillips, M. Donelan, M. Banner, W. Drennan, P. Sullivan, J. McWilliams, M. Parlange, C. Higgins, and C. Meneveau contributed to this work. We gratefully acknowledge the support by the Office of Naval Research, ONR N00014-02-1-0872.

References

Belcher, S. and J. C. R. Hunt: 1993, Turbulent shear flow over slowly moving waves. *J. Fluid Mech.*, **251**, 109–148.

Chalikov, D. and V. Makin: 1991, Models of the wave boundary layer. *Boundary-Layer Meteorology*, **56**, 83–99.

Davis, R. E.: 1969, On high reynolds number flow over a wavy boundary. *J. Fluid Mech.*, **36**, 337–346.

Dobson, F.: 1971, Measurements of atmospheric pressure on wind-generated sea waves. *J. Fluid Mech.*, **48**, 91–127.

Donelan, M. A.: 1999, *Wind Induced Growth and Attenuation of Laboratory Waves*, Clarendon Press, Oxford. 183–194.

Elliott, J.: 1972, Microscale pressure fluctuations near waves being generated by wind. *J. Fluid Mech.*, **54**, 427–448.

Gent, P. R. and P. A. Taylor: 1976, A numerical model of the air flow above water waves. *J. of Fluid Mech.*, **77**, 105–128.

Hare, J., T. Hara, J. Edson, and J. Wilczak: 1997, A similarity analysis of the structure of airflow over surface waves. *Journal of Physical Oceanography*, **27**, 1018–1037.

Hasselmann, D. and J. Bösenberg: 1991, Field measurements of wave-induced pressure over wind sea and swell. *J. Fluid Mech.*, **230**, 391–428.

Hristov, T., C. Friehe, and S. Miller: 1998, Wave-coherent fields in air flow over ocean waves: Identification of cooperative behavior buried in turbulence. *Phys. Rev. Letters*, **81**, 5245–5248.

Hristov, T., S. Miller, and C. Friehe: 2003, Dynamical coupling of wind and ocean waves through wave-induced air flow. *Nature*, **422**, 55–58, doi:10.1038/nature01382.

Lin, C.: 1955, *The theory of hydrodynamic stability*. Cambridge University Press, Cambridge.

Meirink, J. F. and V. Makin: 2000, Modelling low-Reynolds-number effects in the turbulent air flow over water waves. *J. Fluid Mech.*, **415**, 155–174.

Miles, J. W.: 1957, On the generation of surface waves by shear flows. *J. Fluid Mech.*, **3**, 185–204.

Papadimitrakis, Y. A., E. Y. Hsu, and R. L. Street: 1986, The role of wave-induced pressure fluctuations in the transfer processes accross an air-water interface. *J. Fluid Mech.*, **170**, 113–137.

Phillips, O. M.: 1957, On the generation of waves by turbulent wind. *J. Fluid Mech.*, **2**, 417–445.

Shemdin, O. and E. Y. Hsu: 1967, Direct measurement of aerodynamic pressure above a simple progressive gravity wave. *J. Fluid Mech.*, **30**, 403–416.

Snyder, R., F. Dobson, J.A.Elliott, and R. Long: 1981, Array measurements of atmospheric pressure fluctuations above surface gravity waves. *J. Fluid Mech.*, **102**, 1–59.

Snyder, R. L.: 1974, A field study of wave-induced pressure fluctuations above surface gravity waves. *J. Marine Research*, **32**, 497–531.

Sullivan, P. and J. McWilliams: 2002, Turbulent flow over water waves in the presence of stratification. *Physics of Fluids*, **14**, 1182–1195.

Sullivan, P., J. McWilliams, and C.-H. Moeng: 2000, Simulation of turbulent flow over idealized water waves. *J. Fluid Mech.*, **404**, 47–85.

Wyngaard, J.: 1992, Atmospheric turbulence. *Annual Review of Fluid Mechanics*, **24**, 205–233.

Wyngaard, J. C.: 1998, Convection viewed from a turbulence perspective. *Buoyant Convection in Geophysicsl Flows*, E. Plate, E. E. Fedorovich, D. X. Viegas, and J. C. Wyngaard, eds., Kluwer, NATO Advanced Science Institute Series, 23–39.